

This article was downloaded by:

On: 16 January 2011

Access details: *Access Details: Free Access*

Publisher *Taylor & Francis*

Informa Ltd Registered in England and Wales Registered Number: 1072954 Registered office: Mortimer House, 37-41 Mortimer Street, London W1T 3JH, UK



Journal of Energetic Materials

Publication details, including instructions for authors and subscription information:

<http://www.informaworld.com/smpp/title~content=t713770432>

The effects of radiation on (1,3,5 - triamino - 2,4,6 - trinitrobenzene) TATB studied by time-of-flight secondary ion mass spectrometry

J. W. McDonald^{ab}; T. Schenkel^{ab}; M. W. Newman^{ab}; G. Overturf^{ab}; H. Gregg^{ab}; T. R. Niedermayr^{ab}; A. V. Barnes^{ab}; D. H. G. Schneider^{ab}; I. A. Mowat^c; A. V. Hamza^{ab}

^a Lawrence Livermore National Laboratory, ^b Physics Department, Livermore, CA ^c Charles Evans & Associates,

To cite this Article McDonald, J. W. , Schenkel, T. , Newman, M. W. , Overturf, G. , Gregg, H. , Niedermayr, T. R. , Barnes, A. V. , Schneider, D. H. G. , Mowat, I. A. and Hamza, A. V.(2001) 'The effects of radiation on (1,3,5 - triamino - 2,4,6 - trinitrobenzene) TATB studied by time-of-flight secondary ion mass spectrometry', *Journal of Energetic Materials*, 19: 2, 101 – 118

To link to this Article: DOI: 10.1080/07370650108216122

URL: <http://dx.doi.org/10.1080/07370650108216122>

PLEASE SCROLL DOWN FOR ARTICLE

Full terms and conditions of use: <http://www.informaworld.com/terms-and-conditions-of-access.pdf>

This article may be used for research, teaching and private study purposes. Any substantial or systematic reproduction, re-distribution, re-selling, loan or sub-licensing, systematic supply or distribution in any form to anyone is expressly forbidden.

The publisher does not give any warranty express or implied or make any representation that the contents will be complete or accurate or up to date. The accuracy of any instructions, formulae and drug doses should be independently verified with primary sources. The publisher shall not be liable for any loss, actions, claims, proceedings, demand or costs or damages whatsoever or howsoever caused arising directly or indirectly in connection with or arising out of the use of this material.

The Effects of Radiation on (1,3,5 - triamino - 2,4,6 - trinitrobenzene)

TATB studied by Time-of-Flight Secondary Ion Mass

Spectrometry

J. W. McDonald¹, T. Schenkel, M. W. Newman, G. Overturf, H. Gregg, T. R.

Niedermayr, A. V. Barnes, D. H. G. Schneider, Ian A. Mowat* and A. V. Hamza

Lawrence Livermore National Laboratory²

*Charles Evans & Associates³

ABSTRACT

Highly Charged Ion (HCI) Time-of-Flight (TOF) Secondary Ion Mass Spectrometry (SIMS) has been employed to analyze the changes in the surface composition of TATB caused by low energy electron, ultraviolet, and Gamma ray irradiation. Comparisons are made between canary yellow (not irradiated) TATB and TATB that has been "greened" by exposure to radiation. We ascribe the color change from yellow to green to a loss of oxygen. Another striking aspect of this study is the presence of a feature at $m/z = 30$ (NO^+) for highly charged ion SIMS, which does not occur in singly charged ion TOF SIMS.

PACS numbers 33.15.ta, 34.50.Dy

¹ Corresponding author Tel. (925) 422 9067, Fax. (925) 422 5940, e-mail mcdonald6@llnl.gov

² Physics Department, L-414, Livermore, CA 94550

³ 810 Kifer Road, Sunnyvale, CA 94086

Journal of Energetic Materials Vol. 19, 101-118 (2001)
Published in 2001 by Dowden, Brodman & Devine, Inc.

1 INTRODUCTION

Triaminotrinitrobenzene (TATB) has generated considerable interest because it requires substantially more energy to detonate than other energetic materials. This property reduces the hazard and vulnerability and increases the safety of TATB. TATB has been known for its unusual thermal properties since the 1950s. Pristine TATB ($C_6H_6N_6O_6$ mass = 258.03 amu) is canary yellow, but has been observed to turn from yellow to green when exposed to light over time [1]. The color change has no apparent effect on the exothermic performance, but green TATB is slightly less thermally stable than yellow TATB [3]. While this color change can be produced by exposure to ultraviolet light [5, 6], electron irradiation and gamma radiation [6], the radiation damaging processes involved have not been well understood. The question of why canary yellow TATB turns green upon irradiation has been a long-standing question in the high explosive community [4-6].

It has been proposed by Manaa et al. [2] that this color change from yellow to green is due to a loss of oxygen from the TATB molecule forming a nitroso-derivative. Nitroso-derivatives are known to produce color changes in other energetic materials samples [2]. This oxygen loss driven by photon absorption scenario is depicted in figure 1, where pristine TATB absorbs a photon inducing the loss of an oxygen atom and continued photon absorption leads to the loss of more oxygen. The mono-nitroso derivative of TATB has been observed during shock and thermal decomposition experiments [7].

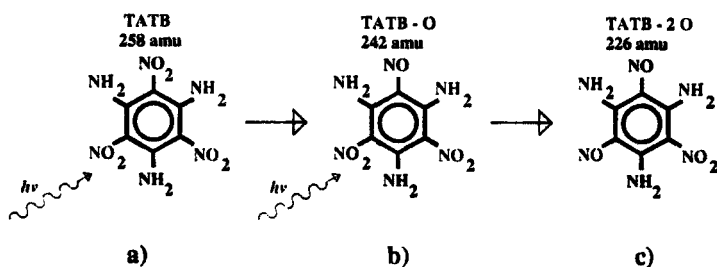


Figure 1 Photon induced loss of oxygen in TATB. Pristine a) [TATB] molecule absorbs a photon and loses an oxygen atom becoming b) [TATB-O]. This process is repeated resulting in c) [TATB-2O].

Britt et al. [8] have used electron spin resonance (ESR) to confirm that free radical production accompanies the color change from yellow to green or black upon exposure to ultraviolet radiation or sunlight although a weaker free radical signal has also been observed in the unirradiated material. The solid free radical is unusually stable (24 months at room temperature). They also used dimethylsulfoxide and dimethylformamide to extract a dissolved free radical from exhaustively photo-irradiated solid TATB that they refer to as a simple H-atom adduct of TATB. Very little of the solid free radical could be extracted and there is no evidence that the dissolved free radical was the same as the solid free radical. A second free radical product was extracted from photolyzed TATB[8]. In the ESR spectrum no hydrogen splitting could be resolved, however a nitrogen splitting of 0.17 gauss was observed for this free radical. The production of free

radicals due to Gamma irradiation was also observed by Miles et al. [6]. The ESR spectrum showed the same singlet at $g = 2.0044$ as observed by Britt et al. in the solid sample. Firsich and Guse [9] have calculated the electron density for the highest occupied molecular orbital for the H-adduct radical. The calculations showed the unpaired electron would remain principally on the NO_2H group, resulting in only one large coupling constant. Since this coupling constant was not observed the H-adduct radical remains controversial.

X-ray photoelectron spectroscopy (XPS) has been applied to the study of the changes of TATB structure upon UV irradiation and shock decomposition [4,5]. In both studies three peaks are observed in the N(1s) region. The peak at 399.0 eV is assigned to the amine nitrogen and the peak at 404 eV is assigned to the nitro group nitrogen. A satellite peak is observed at 407.2 eV. The nitro N(1s) feature and the satellite feature decrease slightly with exposure to UV light and decrease less than 5% upon shocking the sample. The satellite line is observed only on amine substituted trinitrobenzenes. No satellite is observed for trinitrobenzene.

2 EXPERIMENTAL

The highly charged ion experimental set up consists of a secondary ion mass spectrometer [10] in a UHV target chamber attached to an Electron Beam Ion Trap (EBIT) [11] used as a source of slow highly charged ions. The mass resolution of our reflection geometry time-of-flight analyzer system is $\approx 2000 (m/\Delta m)$. The EBIT and its associated beam lines supply momentum analyzed ions in single charge states of various

species, charges, and energies. In the experiment discussed here $^{136}\text{Xe}^{47+}$ and $^{136}\text{Xe}^{44+}$ with kinetic energies of 658 and 616 keV respectively were delivered to the sample targets. In addition to their kinetic energies, these ions also carry potential energies due to their charges of 75 and 51 keV respectively. The interaction of these highly charged ions with surfaces has been studied extensively [12] and is known to cause an enhanced ejection of surface material. This ejected material is composed of positive and negative ions, clusters of ions, and neutrals from the first few atomic layers of the surface. Either positively or negatively charged surface material emitted from the target can be focused into a time-of-flight spectrometer. The spectra discussed in this paper are representations of accumulations of positively charged surface material collected event-by-event. An event is started as a primary analyzing ion (i.e., $^{136}\text{Xe}^{47+}$) impacts the surface. The start signal is the high yield of protons (~50% start efficiency) upon highly charged ion impact. The stop signal is the arrival of a positively charged secondary ion. The primary ion flux is kept below 1000/s to reduce temporally overlapping primary ion events and the beam was apertured to a 1 mm spot size. For each primary ion impinging on the target, the flight time for secondary ion arrival is recorded. After the experiment, the data is analyzed in two ways. First, all events are histogrammed yielding a spectrum comparable to normal TOF SIMS [13], except that the secondary ion yield is much higher [11, 14]. Second, the events are analyzed by histogramming only selected events, such as events that have NO^+ in the list. This feature of HCI TOF SIMS [14] is possible due to the high secondary ion yield per incident HCI (order of one). The secondary ion yield in standard TOF SIMS is much lower per incident ion (order of 10^{-3}). The most striking feature observed in HCI TOF SIMS from TATB samples is the strong signal at

$m/z = 30$ (NO^+), see the bottom of figure 2. This feature is not observed in conventional singly charged ion TOF SIMS on these samples as is shown on the top of the figure. This is due to the higher ionization probability for desorption with highly charged ions. In addition, TATB fragment secondary ions are observed to be highly correlated with this NO^+ feature. The high correlation between the NO^+ feature and the TATB fragments could be due to the molecular fragmentation of an initially double charged species into two positively charged, highly correlated secondary ions that can be detected.

For comparison, an experiment with singly charged gallium ions was performed on a similar target to identify the exact mass defect and differentiate between TATB – O and TATB – NH_2 . A Phi TRIFT II TOF-SIMS instrument was used to collect singly charged time-of-flight secondary ion mass spectrum from the TATB samples at Charles Evans and Associates. Data were obtained using a liquid metal gallium primary ion source with 2 nA beam current. The instrument was operated in an ion microprobe mode (spot size 10 μm) in which the bunched, pulsed primary beam is rastered across the sample's surface. The mass resolution of the Phi TRIFT II was 6700 ($m/\Delta m$) allowing determination of the exact mass of the secondary ions in most cases.

The 5 mg samples of powdered TATB were obtained from the high explosive application facility (HEAF) at LLNL. The powders were pressed between native oxide covered pieces of silicon to produce the targets for analysis. The deposits on the silicon wafers were a mixture of particles and smears. The target wafers were then placed in ultrahigh vacuum to be analyzed. The "yellow" as received (pristine) TATB was kept in the dark as much as possible during handling, however exposure to light was uncontrolled before

receipt. The “green” TATB was produced by irradiation with 70 Mrad Gamma radiation at Los Alamos National Laboratory. The “black” TATB was produced by uncontrolled exposure to a Xe UV lamp. The electron beam exposure used in this study was performed *in situ* with 500 eV electrons at $0.2 \mu\text{A}/\text{mm}^2$ for 600 seconds.

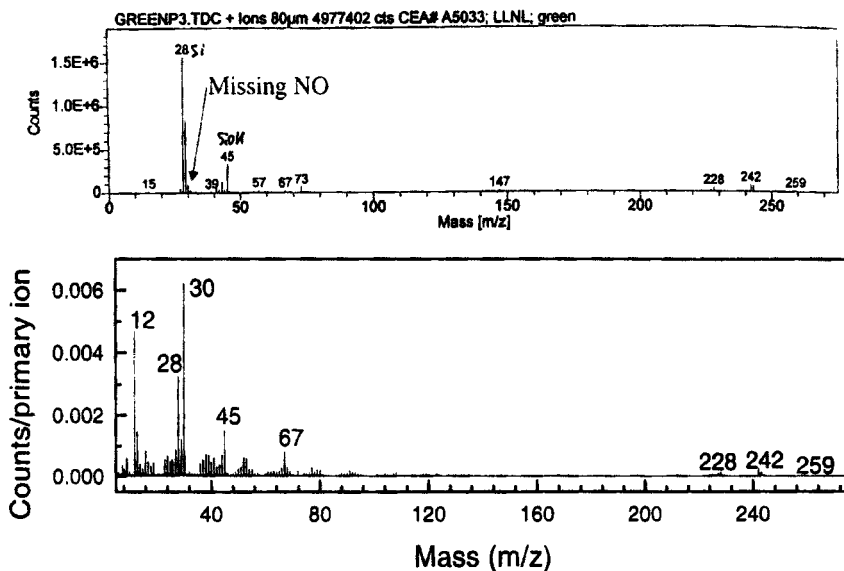


Figure 2 Time of Flight Spectra Showing Feature at $m/z = 30$. The top histogram is from a single charged ion TOF SIMS features masses 28 and 29 while the bottom HCI TOF SIMS histogram features masses 28, 29 and 30.

3 Results and Discussion

The “yellow” as received TATB has been analyzed with HCI TOF SIMS and singly charged TOF-SIMS. The bottom trace in figure 3 shows the HCI TOF SIMS spectrum

collected for the “yellow “control TATB sample in the mass range from 200 to 270 amu. It is highly unlikely that it is possible to observe the secondary ion mass spectrum from pristine TATB alone. First, the primary ions, both highly charged and singly charged, deposit electronic energy into the target. Electronic excitation occurs on a femtosecond time scale [12], which is much faster than the secondary ions can desorb from the surface. As a result, the primary ion radiation can lead to an alteration of the material. However in HCI TOF SIMS the flux of primary ions is kept low so that spatial overlap is exceedingly small. Second, some handling of the TATB is likely to have occurred in ambient light conditions and the ambient light conditions might have produced a change in the surface structure. No discernible change in the color of the control sample was observed after HCI TOF SIMS and singly charged ion TOF-SIMS, however, an altered thin molecular layer can not be ruled out.

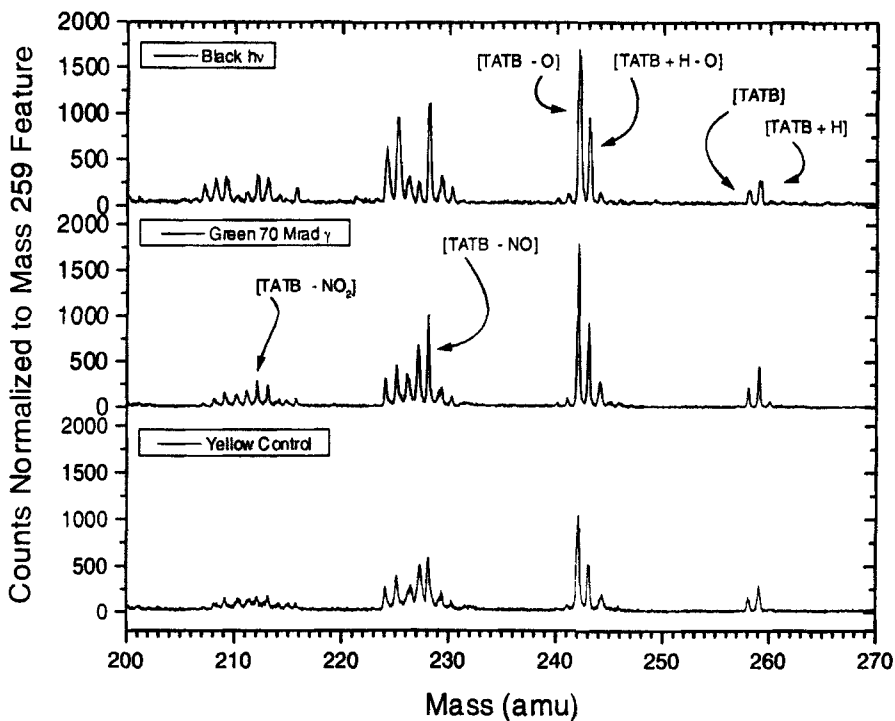


Figure 3 Comparison of yellow TATB (as received) (bottom) and green, Gamma irradiated TATB (70 Mrad) (middle) and black, UV irradiated TATB (top). The Primary ion used in these TOF-SIMS measurements was Xe^{47+} . The y coordinate is normalized counts, where the number of counts in the 259 amu feature (parent TATB) are scaled to be equal.

The largest feature observed in figure 3 is at 242 amu. This feature was also the largest observed in the singly charged TOF-SIMS in the same range. The mass resolution theoretically needed to distinguish TATB-O from TATB-NH₂ is about 10,169. The measured mass resolution of m/z 242 was 6,700 $m/\Delta m$ or 8,040 $t/\Delta t$. However this does not mean that the ion at m/z 242 cannot be identified if sufficient mass accuracy is available. The spectrum are calibrated with low mass hydrocarbons which means that the ion at m/z 242 differs from TATB-O by 9 mDa and from TATB-NH₂ by - 14.8 mDa. However by including the KNOWN ion TATB+H in the calibration, then these differences drop to 1.3 mDa for TATB-O and increase to -22.5 mDa for TATB-NH₂. So that on the balance of probabilities, the ion at m/z 242 is much more likely to be TATB-O than TATB-NH₂. The FWHM peak width of m/z 242 is 21 channels (i.e., 2.898 nsec) and a mass deviation of 22.5 mDa corresponds to 14 channels (1.932 nsec) at this mass to charge ratio. Thus for a peak of sufficient signal to noise ratio acquired with a sufficiently high time channel resolution (138 psec per channel), the centroid can be accurately measured, even with lower than the theoretically necessary mass resolution. A difference in peak position of 1.932 nsec can easily be measured with a mass resolution of 6,700. Therefore, the 242 amu feature is assigned to TATB minus oxygen [TATB-O]. Other features observed in the control TATB sample are at 243 amu (parent minus O+H [TATB-O+H]), 258 amu (parent [TATB]), 259 amu (parent plus H [TATB+H]), 228 amu

(parent minus NO [TATB-NO]), 227 amu (parent minus O₂ plus H [TATB-O₂+H]), 225 amu (parent minus O₂H [TATB-O₂H]), and 224 amu (parent minus O₂H₂ [TATB-O₂H₂]). The fragmentation is due to the primary ion irradiation and/or sample structure. The addition of a proton is likely due to stabilization of the secondary ions, since protons are readily available during the desorption process.

The appearance of the [TATB-NO] feature at 228 amu is quite striking. In order to form this ion, the TATB molecule has to undergo a molecular rearrangement. A possibility would be that the NO from a nitro group desorbs and the other oxygen atom from the nitro reattaches at the carbon atom. The 228 amu ion feature is highly correlated with the NO⁺ feature in coincidence counting, indicating these two secondary ions come from the same desorption event. The mass calculation described above can rule out the removal of NO₂ and the addition of NH₂ to form a feature with mass 228 amu.

The trace in the middle of figure 3 shows differences in the HCI-TOF-SIMS spectrum due to 70 Mrad Gamma irradiation. At first glance the green spectrum looks remarkably similar to the yellow control spectrum. This is likely due to the supposition that the surface of the yellow control sample has irradiated slightly in handling. The 242 amu and the 243 amu features are larger in the Gamma irradiated sample, indicating higher oxygen loss in the green sample. The minus NO feature at 228 amu and the minus NO₂ feature at 212 amu are also larger.

The trace at the top of figure 3 shows differences in the HCl-TOF-SIMS spectrum due to UV irradiation. Besides the increases in the oxygen loss features at 242 and 243 amu, there is increased signal in the double and triple oxygen loss features at 224, 225, 209, 208, and 207 amu. Similar increases in the minus NO and minus NO₂ features at 228 and 212 amu are observed as with Gamma irradiation.

After the initial analysis, the yellow control target was exposed to 500 eV electrons with a current density of 0.2 $\mu\text{A}/\text{mm}^2$ for 600 seconds and reanalyzed *in situ*. The comparison of the as-received TATB spectrum to the electron beam irradiated TATB spectrum are shown in figure 4. The parent (TATB) features at 258 and 259 amu are absent after electron beam bombardment. The figure also shows an increase in both the TATB – NO (228 amu) and the TATB- NO₂ (212 amu) after electron bombardment. Also shown in the figure is a decrease in the feature at TATB-O (242 amu).

The changes observed in the spectrum are due to the electronic excitation by the incident electrons, since the exposure of the control sample to the highly charged ion beam was less than 10^8 ions and the sample did not show any changes during analysis. The probability of spatial overlap is small with the small number of ions over a relatively large area ($\cong 3\text{mm}$ in diameter). The energy of the electron beam is sufficient to produce core holes in the nitrogen atoms, but not the oxygen atoms. Localization of a hole on the nitrogen atom may lead to desorption of the nitro group. If the minus oxygen feature at 242 amu is a nitroso derivative, localization of a core hole on the nitroso nitrogen could lead to desorption of the nitroso group and hence the decrease in the 242 feature as well.

This type of behavior would *not* be expected for ultraviolet radiation. The energy would not be sufficient to excite a core hole. However, UV radiation and lower energy electrons could excite the valence band. The lowest energy peak in the valence band is comprised primarily of orbitals localized on the nitro group and made up from oxygen 2p atomic orbitals [5]. Removal of electrons from this band will weaken the N-O bond and hence may lead to the desorption of oxygen. This molecular orbital also contains $n = 2p$ atomic orbitals and could lead to desorption of the NO and NO₂. However, the faster lighter oxygen may be able to leave the molecule before it deexcites, statistically more often than the heavier, slower, NO and NO₂.

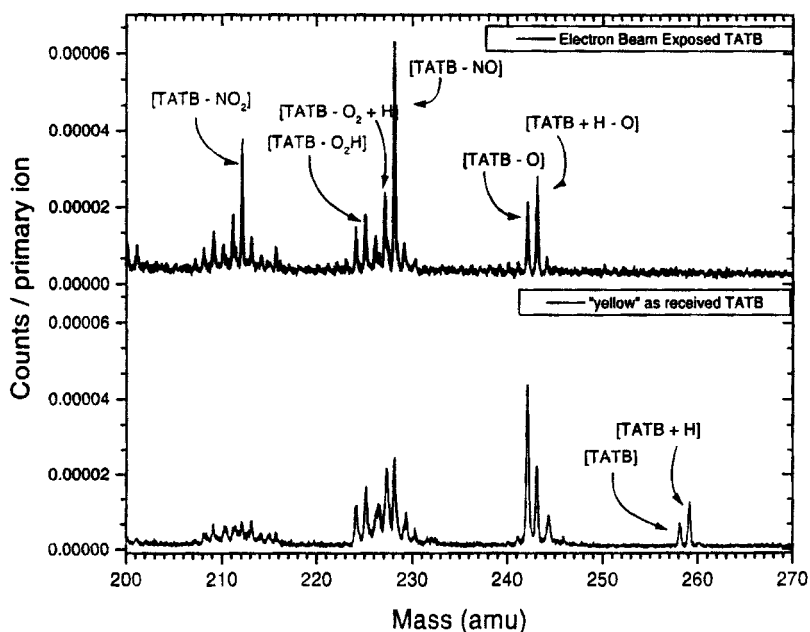


Figure 4 Comparison of yellow TATB (as received) (bottom) and electron beam irradiated TATB (top).

The Primary ion used in these TOF-SIMS measurements was Xe^{47+} . The y-coordinate is counts per primary ion.

In addition, molecules below the first molecular layer transport of the smaller oxygen may be more facile. However, the interlayer spacing in TATB is quite large, 3.23Å, and should be able to accommodate a nitro group or NO as well as oxygen. Both the core hole initiated, and the valence hole initiated desorption mechanisms would be expected for Gamma irradiation since any high energy electrons liberated would quickly cascade down to low energy electrons.

The increase in the 242 amu feature for the green Gamma irradiated sample and the black UV irradiated sample would be consistent with the mechanism of greening proposed by Manaa et al. [2], in that the 242 amu feature would be associated with the mono-nitroso derivative of TATB. The loss of more oxygen would lead to di nitroso or tri nitroso derivatives of TATB.

The nitroso greening mechanism must be reconciled with the x-ray photoelectron (XP) results [4,5] and the electron spin resonance results [6,8]. If the nitroso is formed it should have a signature in the XP spectrum. Perhaps this is the source of the satellite feature. Removal of an oxygen from the nitro group could leave a multiple bond between the remaining oxygen and nitrogen analogous to the radical NO. This would leave a free radical on the bond that could reconcile the ESR spectrum of Britt *et al.* [8] (see below). The 2p electrons would be spatially moved away from the nitrogen towards the remaining oxygen. Decreased electron density on the nitrogen may shift the N 1s binding

energy to higher values (the satellite is at 2.8 eV higher binding energy) in agreement with Distefano et. al. [16].

Removal of an oxygen from the nitro group may leave a free radical on the nitroso group [17]. This could be the type of free radical observed in the ESR measurements [8] where $g=2.0044$. The observed g factors for nitroso compounds complexed with silver II vary from 2.0047 to 2.0055 [17]. The shift of 0.0003 may be due to the presence of the amine groups in TATB or the absence of silver II.

Hence, many (if not all) of the measurements could be reconciled, including shock measurements [9, 10] that show a loss of oxygen. The fact that nitro group desorption is observed as well [5, present work] serves to cloud the picture. The nitro desorbs, but perhaps not as readily, and may not give rise to the green color.

The irradiation of TATB with electrons, UV photons and Gamma radiation leads to both the loss of oxygen and to the loss of nitro groups from the molecule. The oxygen desorption may be more facile. The green color of the irradiated material could likely be due to the formation of a mono-nitroso derivative of TATB.

Acknowledgments

The authors wish to acknowledge the technical assistance of Edward Magee for his assistance in setting up this experiment, and Greg Buntain of LANL for the Gamma-irradiated TATB. This work performed under the auspices of the U.S. Department of Energy by University of California Lawrence Livermore National Laboratory under contract No. W-7405-Eng-48.

References

- [1] A. Chien, G. Overturf, and J. LeMay, The Greening of 1,3,5-Triamino-2,4,6 trinitrobenzene (TATB): A Literature Review. UCRL-UR-136724.
- [2] M. Manaa, R. Schmidt, G. Overturf, B. Watkins, L. Fried, and J. Kolb, Report, Lawrence Livermore National Laboratory, UCRL-ID-134559.
- [3] M. F. Foltz, D. L. Ornellas, P. F. Pagoria, A. R. Mitchell, *Journal of Materials Science* **31**, 1893 (1996).
- [4] P. S. Wang and T. N. Wittberg, *J. Mater. Sci.* **24**, 1533 (1989).
- [5] J. Sharma, W. L. Garrett, F. J. Owens, and V. L. Vogel, *J. Phys. Chem.* **86**, 1657 (1982); J. Sharma and F. J. Owens, *Chem. Phys. Lett.* **61**, 280 (1979); J. Sharma, J. C. Hoffsommer, D. J. Glover, C. S. Coffey, F. Santiago, A. Stolovy, and S. Yasuda in *Shock Waves in Condensed Matter*, Editor(s): J. R. Asay, R.A. Graham, and G. K. Straub, (North-Holland, Amsterdam, Neth.) 543 (1984).
- [6] M. Miles, D. Gustaveson, and K. Devries, *J. Mater. Sci.* **18**, 3243 (1983).
- [7] H. Ostmark, in *Shock Compression of Condensed Matter*, edited by S. C. Schmidt and W. C. Tao 871 (AIP Press, 1996).
- [8] A. D. Britt, W. B. Moniz, G. C. Chingas, D. W. Moore, C. A. Heller, and C. L. Ko, *Propellants and Explosives* **6**, 94 (1981).
- [9] D. W. Firsich and M. P. Guse, *Journal of Energetic Materials* **2**, 205 (1984).

- [10] T. Shenkel, A. V. Barnes, N. W. Newman, G. Machicoane, T. Niedermayer, M. Hattass, J. W. McDonald, D. H. Schneider, K. J. Wu and R. W. Odom, *Physica Scripta*, **T80**, 73 (1999).
- [11] D. Schneider, M. W. Clark, B. M. Penetrante, J. McDonald, D. Dewitt, and J. N. Bardsley, "Production of high-charge-state thorium and uranium ion in an electron-beam ion trap", *Phys. Rev. A* **44**, 3119 (1991).
- [12] T. Schenkel, A. V. Hamza, A. V. Barnes, D. H. Schneider, "Interaction of slow, very highly charged ions with surfaces", *Progress in Surface Sciences* **61**, 23 (1999).
- [13] A. Benninghoven and L. Wiedmann, *Surface Science* **41**, 483 (1974).
- [14] A. V. Hamza, T. Schenkel, A. V. Barnes, and D. H. Schneider, *Journal of Vacuum Science and Technology A* **17**, 303 (1999).
- [15] Hans Ågren and Björn O. Roos, Paul S. Bagus, Ulrik Gelius, Per-Åke Malmquist, Svante Svensson, Rein Maripuu, and Kai Siegbahn, *J. Chem. Phys.* **77** 3893 (1982).
- [16] Giuseppe, Derek Jones, Alberto Modelli, Salvatore Piganatro, *Physica Scripta*, **16**, 373 (1977).
- [17] A. Jezierski, *Magnetic Resonance in Chemistry* **27**, 130 (1989).